

Analyses of turbulence in a wind tunnel by a multifractal theory for probability density functions

Toshihico Arimitsu^{1‡}, Naoko Arimitsu² and Hideaki Mouri³

¹Faculty of Pure and Applied Sciences, University of Tsukuba, Tsukuba, Ibaraki 305-8571, JAPAN

²Faculty of Environment and Information Sciences, Yokohama National University, Yokohama, Kanagawa 240-8501, JAPAN

³Meteorological Research Institute, Tsukuba, Ibaraki 305-0052, JAPAN

E-mail: arimitsu.toshi.ft@u.tsukuba.ac.jp

Abstract. The probability density functions (PDFs) for energy dissipation rates created from turbulence in a wind tunnel, are analyzed by multifractal probability density function theory, and the validity of the new scaling relation is proven in the case of experimental turbulence. The tail part of PDF, representing intermittent coherent motion in fully developed turbulence, is determined by Tsallis-type PDF for singularity exponents with the new scaling relation which shows that the coherent motion is deeply related to the marginal instabilities within a dynamical system at the δ^k -period ($\delta > 2$) saddle-node bifurcation points ($k = 1, 2, 3, \dots$) associated with δ^k -period windows constituting a self-similar nesting structure. For the central part PDF representing both contributions from the coherent motion and the fluctuating motion twining around the former, we introduced a trial function specified by three adjustable parameters which reveal scaling behaviors in much wider area not restricted to the inertial range. The connection point between the central and tail parts of PDF provides us with an important information to distinguish the characteristics of the two motions. A trial is performed how to extract the information of incoherent motion with the help of two different ways in creating PDFs from the observed time-series data.

Keywords: Multifractal, Fat tail, Intermittency, Turbulence, Energy dissipation rates

‡ Corresponding author: arimitsu.toshi.ft@u.tsukuba.ac.jp

1. Introduction

There are several keystone works (Mandelbrot 1974, Parisi and Frisch 1985, Benzi *et al* 1984, Halsey *et al* 1986, Meneveau and Sreenivasan 1987, Nelkin 1990, Hosokawa 1991, Benzi *et al* 1991, She and Leveque 1994, Dubrulle 1994, She Z-S and Waymire 1995, Arimitsu T and N 2000a, 2000b, 2001, 2002, Arimitsu N and T 2002, Biferale *et al* 2004, Chevillard *et al* 2006) providing the multifractal aspects for fully developed turbulence. Only a few works (Benzi *et al* 1991, Arimitsu T and N 2001, 2002, Arimitsu N and T 2002, Biferale *et al* 2004, Chevillard *et al* 2006) analyze the probability density functions (PDFs) for physical quantities representing intermittent character. The other works deal with only the scaling property of the system, e.g., comparison of the scaling exponents of velocity structure function. Among the researches analyzing PDFs, multifractal probability density function theory (MPDFT) (Arimitsu T and N 2001, 2002, 2011, Arimitsu N and T 2002, 2011) provides the most precise analysis of the fat-tail PDFs. MPDFT is a statistical mechanical ensemble theory constructed by the authors (T.A. and N.A.) in order to analyze intermittent phenomena providing fat-tail PDFs.

To extract the intermittent character of the fully developed turbulence, it is necessary to have information of self-similar hierarchical structure of the system. This is realized by producing a series of PDFs for responsible singular quantities with different lengths

$$\ell_n = \ell_0 \delta^{-n}, \quad \delta > 1 \quad (n = 0, 1, 2, \dots) \quad (1)$$

that characterize the regions in which the physical quantities are coarse-grained. The value for δ is chosen freely by observers. Let us assume that the self-similar structure of fully developed turbulence is such that the choice of δ should not affect the theoretical estimation of the values for the fundamental quantities characterizing the turbulent system under consideration. A&A model within the framework of MPDFT itself tells us that this requirement is satisfied if the scaling relation has the form (Arimitsu T and N 2011, Arimitsu N and T 2011)

$$\ln 2 / (1 - q) \ln \delta = 1 / \alpha_- - 1 / \alpha_+. \quad (2)$$

Here, q is the index associated with the Rényi entropy (Rényi 1961) or with the Havrda-Charvat and Tsallis (HCT) entropy (Havrda and Charvat 1967, Tsallis 1988); α_{\pm} are zeros of the multifractal spectrum $f(\alpha)$ (see below in section 2). The multifractal spectrum is uniquely related to the PDF for α (see (4) below). The PDF of α is related to the tail part of PDFs within MPDFT for those quantities revealing intermittent behavior whose singularity exponents can have values $\alpha < 1$, e.g., the energy dissipation rates, through the variable transformation between α and the physical quantities (see (3) below for the case of the energy dissipation rates ε_n). With the new scaling relation (2), observables have come to depend on the parameter δ only in the combination $(1 - q) \ln \delta$. The difference in δ is absorbed in the entropy index q . §

§ Since almost all the PDFs that had been provided previously were for the case where $\delta = 2$, it has been possible to analyze PDFs (Arimitsu T and N 2001, 2002, Arimitsu N and T 2002) with the scaling

Table 1. Parameters of turbulence in the wind tunnel (Mouri *et al* 2008). The inertial range is determined as the region where the second moment of the velocity differences for longitudinal component scales with the exponent $2/3$ with respect to the distance between the positions of two velocities used to derive the velocity difference. Measurements are performed on the centerline of tunnel by a hot-wire anemometer with a crossed-wire probe. It is expected that turbulence around the probe is homogeneous in both stream-wise and span-wise directions as the cross section of a lattice constituting the grid is small enough compared with that of the tunnel.

Quantity	Value
Microscale Reynolds number Re_λ	409
Kolmogorov length η	0.138 mm
Kinematic viscosity ν	$1.42 \times 10^{-5} \text{ m}^2 \text{ sec}^{-1}$
Mean velocity of downstream wind U	21.16 m sec^{-1}
Mean energy dissipation rate $\langle\langle \varepsilon \rangle\rangle = 15\nu\langle\langle (\partial v/\partial x)^2 \rangle\rangle/2$	$7.98 \text{ m}^2 \text{ sec}^{-3}$
Correlation length of longitudinal velocity	17.9 cm
Inertial range	$50 \lesssim r/\eta \lesssim 150$
RMS of span-wise velocity fluctuations $\langle\langle v^2 \rangle\rangle^{1/2}$	1.06 m sec^{-1}
RMS of stream-wise velocity fluctuations $\langle\langle u^2 \rangle\rangle^{1/2}$	1.10 m sec^{-1}
Cross section of the wind tunnel	3 m \times 2 m
Separation of the axes of adjacent rods constituting grid	20 cm
Distance of the probe downstream from the grid	4 m
Sampling interval Δt	$1.43 \times 10^{-5} \text{ sec}$
Number of data points	4×10^8

In the preceding papers, we analyzed PDFs for energy transfer rates (Arimitsu T and N 2011) and PDFs for energy dissipation rates (Arimitsu N and T 2011) created from 4096^3 DNS (Aoyama *et al* 2005) with the help of the new scaling relation, and checked the independence of the PDFs from δ . It was found that the adjustable parameters for the central part PDF provide us with δ -independent scaling behaviors as functions of r/η , and that the scaling properties are satisfied in much wider region not restricted to inside of the inertial range. However, we did not have enough resolution (the number of data points in drawing PDFs), at that moment, for the analyses of the central part PDFs performed in Arimitsu T and N (2011) and Arimitsu N and T (2011). We will perform, as one of the aims of the present paper, the same analyses as were done for DNS, with the help of PDFs created from wind tunnel turbulence with a higher enough resolution in order to make sure if the characteristics discovered previously with rather poor resolution at the central part are correct or not. It is possible since we have the raw time-series data taken from wind tunnel turbulence with which we can create PDFs for energy dissipation rates with enough resolutions fit to our needs.

In this paper, we analyze the PDFs for energy dissipation rates extracted out from the time series of the velocity field of a fully developed turbulence which were observed by one of the authors (H.M.) in his experiment conducted in a wind tunnel (Mouri *et al*

relation $1/(1-q) = 1/\alpha_- - 1/\alpha_+$ proposed by Costa *et al* (1998) and Lyra and Tsallis (1998) in the context of dynamical systems.

2008). The information and basic parameters of the turbulence are listed in table 1 for convenience. In section 2, we present the formulae of theoretical PDFs within A&A model which are necessary in the following sections for the analyses of PDFs obtained from the experimental turbulence. In section 3, we analyze the observed PDFs for energy dissipation rates in a high precision with the theoretical PDF within A&A model of MPDFT, and verify the proposed assumption related to the magnification δ . In section 4, in order to see what information we can extract out from the time-series data, we compare two different PDFs for energy dissipation rates created from the time series data with different approximation for temporal derivative. We may learn from this how to treat the central part of PDFs to derive the information of incoherent fluctuating motion around the coherent turbulent motion. Summary and Discussions are provided in section 5.

2. Singularity exponent and PDFs for energy dissipation rates

MPDFT is constructed under the assumption, following Parisi and Frisch (1985), that for high Reynolds number the singularities distribute themselves in a multifractal way in real physical space. The singularities stem from the scale invariance of the Navier-Stokes (N-S) equation for an incompressible fluid under the scale transformation $\vec{x} \rightarrow \vec{x}' = \lambda \vec{x}$ accompanied by the scale changes $\vec{u} \rightarrow \vec{u}' = \lambda^{\alpha/3} \vec{u}$ in velocity field, $t \rightarrow t' = \lambda^{1-\alpha/3} t$ in time and $p \rightarrow p' = \lambda^{2\alpha/3} p$ in pressure with an arbitrary real number α . In treating an actual turbulent system, the value of the kinematic viscosity ν in the dissipation term in N-S equation is fixed to a value unique to the material of fluid prepared for an experiment. In this sense, for the study of fully developed turbulence, we have to look for a coherent turbulent state which is invariant under the above scale transformation accompanied by the dissipation term breaking the invariance. We should keep in mind that the dissipation term can become effective depending on the region under consideration since the term breaking the invariance does exist, i.e., non-zero (see the discussions in the following), and provides us with a specific character of fluctuation around the coherent turbulent motion of fluid.

The energy dissipation rate ε_n averaged in the regions with diameter ℓ_n has the scaling property of the form

$$\varepsilon_n/\epsilon = (\ell_n/\ell_0)^{\alpha-1} \quad (3)$$

where we put $\varepsilon_0 = \epsilon$. Here, we assume that the energy input rate ϵ is constant. The energy dissipation rate has singularities for $\alpha < 1$, i.e., $\lim_{n \rightarrow \infty} \varepsilon_n = \lim_{n \rightarrow \infty} \ell_n^{\alpha-1} \rightarrow \infty$. The degree of singularity is specified by the singularity exponent α (Parisi and Frisch 1985).

Let us consider α to be a stochastic variable, and to be related definitely to the quantity representing intermittent behavior. MPDFT provides us with a systematic framework to make a connection between the distribution of α and the PDFs of observed quantities. Within A&A model of MPDFT (Arimitsu T and N 2000a, 2000b, 2001, 2002,

2011, Arimitsu N and T 2002, 2011), the PDF $P^{(n)}(\alpha)$ for α is given by the Rényi or HCT type function:

$$P^{(n)}(\alpha) \propto [1 - (\alpha - \alpha_0)^2 / (\Delta\alpha)^2]^{n/(1-q)} \quad (4)$$

with $\Delta\alpha = [2X/(1-q)\ln\delta]^{1/2}$. The domain of α is $\alpha_{\min} \leq \alpha \leq \alpha_{\max}$ with α_{\min} and α_{\max} being given by $\alpha_{\min/\max} = \alpha_0 \mp \Delta\alpha$. q is the entropy index. From (4), we have for $n \gg 1$ the expression of the multifractal spectrum

$$f(\alpha) = 1 + \ln [1 - (\alpha - \alpha_0)^2 / (\Delta\alpha)^2] / (1 - q) \ln \delta. \quad (5)$$

The three parameters α_0 , X and q appeared in $P^{(n)}(\alpha)$ are determined as the functions of the intermittency exponent μ with the help of the three conditions. One is the energy conservation law $\langle \varepsilon_n \rangle = \epsilon$. Another is the definition of the intermittency exponent μ , i.e., $\langle (\varepsilon_n / \epsilon)^2 \rangle = (\ell_n / \ell_0)^{-\mu}$. The last condition is the scaling relation (2) with α_{\pm} being the solution of $f(\alpha_{\pm}) = 0$, which is a generalization of the one introduced by Tsallis and his coworkers (Costa *et al* 1998, Lyra and Tsallis 1998) to which (2) reduces when $\delta = 2$. Here, the average $\langle \dots \rangle$ is taken with $P^{(n)}(\alpha)$. The parameter q is determined, altogether with α_0 and X , as a function of μ only in the combination $(1 - q) \ln \delta$. The difference in δ is absorbed into the entropy index q , therefore changing the zooming rate δ may result in picking up the different hierarchy, containing the entropy specified by the index q , out of self-similar structure of turbulence. As the parameters are dependent on q only in the combination $(1 - q) \ln \delta$, we are naturally led to the replacement of n in the expression of $P^{(n)}(\alpha)$ in (4) with $n = \tilde{n} / \ln \delta$. If \tilde{n} does not depend on δ , $P^{(n)}(\alpha)$ becomes also independent of δ . Note that, with the new number \tilde{n} , ℓ_n introduced in (1) reduces to

$$\ell_n = \ell_0 e^{-\tilde{n}}. \quad (6)$$

We are assuming that the probability $\Pi_3^{(n)}(\varepsilon_n) d\varepsilon_n$ can be, generally, divided into two parts as

$$\Pi_3^{(n)}(\varepsilon_n) d\varepsilon_n = \Pi_{3,S}^{(n)}(\varepsilon_n) d\varepsilon_n + \Delta \Pi_3^{(n)}(\varepsilon_n) d\varepsilon_n. \quad (7)$$

The first term describes the coherent motion, i.e., the contribution from the abnormal part of the physical quantity ε_n due to the fact that its singularities distribute themselves multifractal way in real space. This is the part representing a coherent turbulent motion

|| The function (4) is the MaxEnt PDF derived from the Rényi entropy or from the HCT entropy with two constraints, one is the normalization condition and the other is a fixed q -variance (Tsallis 1988). This choice of PDF is also quite natural since the Rényi entropy and the HCT entropy are directly related to the generalized dimension (Hentschel and Procaccia 1983) describing those systems containing multifractal structures (Grassberger 1983). Note that for the HCT entropy the relation is given with the help of the q -exponential (Tsallis 2001) which is a function satisfying a scaling invariance (Suyari and Wada 2006) and reduces to the ordinary exponential for $q \rightarrow 1$.

¶ The introduction of \tilde{n} is intimately related to the infinitely divisible process (Dubrulle 1994, She and Waymire 1995). It is confirmed by the observation in the preset paper that \tilde{n} is independent of δ and has values of $\mathcal{O}(1)$ (see table 2). Then, taking the limit $\delta \rightarrow 1+$ with a fixed value of \tilde{n} , one has an infinitely divisible distribution. A detailed investigation of A&A model from this view point will be given elsewhere in the near future.

given in the limit $\nu \rightarrow 0$ but is not equal to zero ($\nu \neq 0$). The second term represents the contribution from the incoherent fluctuating motion. The normalization of PDF is specified by $\int_0^\infty d\varepsilon_n \Pi_3^{(n)}(\varepsilon_n) = 1$. We assume that the coherent contribution is given by (Arimitsu T and N 2001) $\Pi_{3,S}^{(n)}(\varepsilon_n) d\varepsilon_n = \bar{\Pi}_{3,S}^{(n)} P^{(n)}(\alpha) d\alpha$ with the variable transformation (3). For the expression of $\bar{\Pi}_{3,S}^{(n)}$, see Arimitsu N and T (2011).

Let us introduce another division of the PDF, i.e.,

$$\hat{\Pi}_3^{(n)}(\xi_n) = \hat{\Pi}_{3,cr}^{(n)}(\xi_n) + \hat{\Pi}_{3,tl}^{(n)}(\xi_n), \quad (8)$$

where $\hat{\Pi}_3^{(n)}(\xi_n)$ is introduced by the relation $\hat{\Pi}_3^{(n)}(\xi_n) d\xi_n = \Pi_3^{(n)}(\varepsilon_n) d\varepsilon_n$ with the variable transformation $\xi_n = \varepsilon_n / \langle \varepsilon_n^2 \rangle_c^{1/2}$ where the cumulant average $\langle \cdot \rangle_c$ is taken with the PDF $\Pi_3^{(n)}(\varepsilon_n)$. The two parts of the PDF, the tail part $\hat{\Pi}_{3,tl}^{(n)}(\xi_n)$ and the central part $\hat{\Pi}_{3,cr}^{(n)}(\xi_n)$, are connected at $\xi_n = \xi_n^*$ under the conditions that they have the common value and the common log-slope there. Note that ξ_n^* is related to ε_n^* by $\xi_n^* = \varepsilon_n^* / \langle \varepsilon_n^2 \rangle_c^{1/2}$ and to α^* by (3). The value of α^* is determined for each PDF as an adjusting parameter in the analysis of PDFs obtained by ordinary or numerical experiments.

When one creates a PDF for energy dissipation rates, he puts each realization into an appropriate bin according to the value ε_n which is obtained by averaging the microscopic energy dissipation rates in each time interval corresponding to the length ℓ_n . For larger ε_n values belonging to the tail part domain of the PDF, most of the realizations in a bin at the interval $\varepsilon_n \sim \varepsilon_n + d\varepsilon_n$ come from the time interval containing at least one intermittently large spike (singular spike) of microscopic energy dissipation rates. The bin may have negligibly small proportion of the number of realizations coming from those intervals with only non-singular spikes compared to the number of realizations with at least one singular spike. On the other hand, for smaller ε_n values belonging to the central part PDF domain, the number of realizations coming from the intervals with singular but small spikes is about the same order as the number of realizations from the intervals containing only non-singular fluctuating spikes, since the height of singular spikes contributing to this bin must be about the same height as non-singular spikes. We interpret that the intermittent singular spikes are related to the coherent turbulent motion such as vortexes and eddies, and that the non-singular spikes should be fluctuations, specific to fully developed turbulence, twining around the coherent motion.

Under the above interpretation, it may be reasonable to assume that, for the tail part of PDF $\hat{\Pi}_{3,tl}^{(n)}(\xi_n)$, the contribution from the first term $\Pi_{3,S}^{(n)}(\varepsilon_n)$ in (7) to the intermittent rare events dominates, and the contribution from the second term $\Delta \Pi_3^{(n)}(\varepsilon_n)$ to the events is negligible, i.e.,

$$\hat{\Pi}_{3,tl}^{(n)}(\xi_n) d\xi_n = \Pi_{3,S}^{(n)}(\varepsilon_n) d\varepsilon_n \quad (9)$$

for $\xi_n^* \leq \xi_n$. For $0 \leq \xi_n \leq \xi_n^*$, as there is no theory for the central part of PDF $\hat{\Pi}_{3,cr}^{(n)}(\xi_n)$ at present, we put

$$\hat{\Pi}_{3,cr}^{(n)}(\xi_n) d\xi_n = \bar{\Pi}_3^{(n)} e^{-[g_3(\xi_n) - g_3(\xi_n^*)]} (\ell_n / \ell_0)^{1-f(\alpha^*)} (\bar{\xi}_n / \xi_n^*) d\xi_n \quad (10)$$

with a trial function of the Tsallis-type

$$e^{-g_3(\xi_n)} = (\xi_n/\xi_n^*)^{\theta-1} \times \{1 - (1 - q') [\theta + f'(\alpha^*)] [(\xi_n/\xi_n^*)^{w_3} - 1] / w_3\}^{1/(1-q')} \quad (11)$$

and $\bar{\Pi}_3^{(n)} = \bar{\Pi}_{3,S}^{(n)} \sqrt{|f''(\alpha_0)|/2\pi |\ln(\ell_n/\ell_0)|} / \bar{\xi}_n$. The parameter w_3 is adjusted by the property of the experimental PDFs around the connection point; q' is the entropy index different from q in (4); θ is determined by the property of PDF near $\xi_n = 0$. For the expression of $\bar{\xi}_n$, see Arimitsu N and T (2011). The contribution to $\hat{\Pi}_{3,cr}^{(n)}(\xi_n)$ comes both from coherent and incoherent motions.

The reason why we chose the trial function (11) for the central part PDF is because it is a natural generalization of the χ -square distribution function for the variable $y_n = (\xi_n/\xi_n^*)^{w_3}$. The observed value of q' is in the range $1.03 \leq q' \leq 1.09$ (see table 2). Note that in the limit $q' \rightarrow 1$ the trial function reduces to the χ -square distribution function for y_n . The quantity $(\theta + w_3 - 1)/w_3$ provides us with an estimate for the number of independent degrees of freedom for the dynamics contributing to the central part of PDF.

3. Verification of assumptions through the analyses of experimental PDFs

By means of the theoretical formula within MPDFT summarized in the last section, we analyze PDFs of energy dissipation rates created from the time series data (Mouri *et al* 2008) for turbulence in a wind tunnel (see table 1). Assuming isotropy of the turbulence, we adopted the surrogate $15\nu(\partial v/\partial x)^2/2 = 15\nu(\partial v/\partial t)^2/2U^2$ for the energy dissipation rate (Cleve *et al* 2003, Mouri *et al* 2008) with the mean velocity U of downstream wind (see table 1) where x -axis is chosen to the direction of the mean flow in a wind tunnel and v is the span-wise velocity component (see Mouri *et al* (2008) for detail). Here, we used Taylor's frozen hypothesis in replacing the variable from time t to space x . For the estimation of $\partial v/\partial t$, we use here the relation

$$\partial v/\partial t \simeq \Delta^{(3)}v/\Delta t = \{8 [v(t + \Delta t) - v(t - \Delta t)] - [v(t + 2\Delta t) - v(t - 2\Delta t)]\} / 12\Delta t \quad (12)$$

where Δt is the sampling interval observing velocity (see table 1). With this formula, we can have a better estimate of the velocity time derivative by means of $\Delta^{(3)}v/\Delta t$ without contamination up to the term of $\mathcal{O}(\Delta t)^3$. We represent the *local* energy dissipation rates derived from (12) by the symbol ε , i.e., $\varepsilon = 15\nu(\Delta^{(3)}v/\Delta t)^2/2U^2$.

We are assuming that the turbulence around the probe is isotropic even for larger scales since the values of RMS one-point velocity fluctuations for span-wise and stream-wise components are almost equal (see table 1). There are still possible pitfalls about the assumption of isotropy (Biferale and Procaccia 2005) because of the difference of values between the averaged energy dissipation rates estimated with the span-wise velocity component v , i.e., $15\nu\langle(\partial v/\partial x)^2\rangle/2 = \langle\varepsilon\rangle = 7.98 \text{ m}^2 \text{ sec}^{-3}$, and the one estimated with the stream-wise velocity fluctuation u , i.e., $15\nu\langle(\partial u/\partial x)^2\rangle = 8.58 \text{ m}^2 \text{ sec}^{-3}$ (Mouri

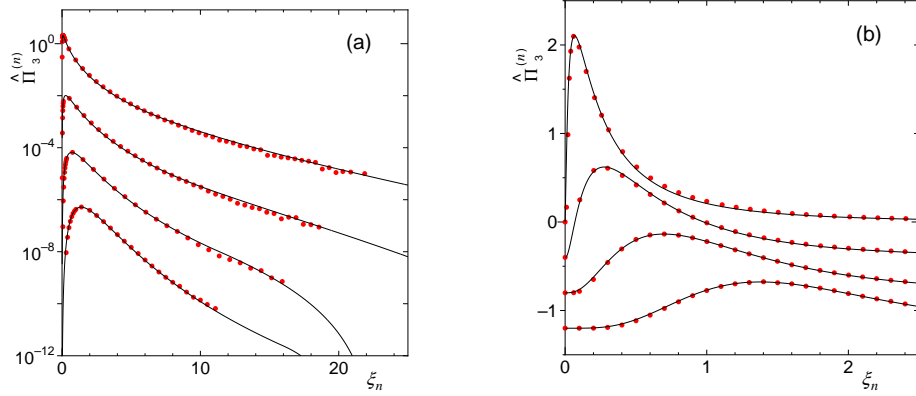


Figure 1. PDFs of energy dissipation rates for $\delta = 3$ on (a) log and (b) linear scale in the vertical axes. For better visibility, each PDF is shifted by -2 unit along the vertical axis in (a) and by -0.4 unit along the vertical axis in (b). Closed circles are the experimental PDFs for $r/\eta = 21.9, 65.7, 197$ and 591 from the smallest value (top) to the largest value (bottom) where r corresponds to ℓ_n . Solid lines represent the curves given by the present theory with parameters listed in table 2 (a).

et al 2008). However, as the difference is less than 10 %, we expect that anisotropy, even if it exists, may not affect the following analyses seriously.

In creating the experimental PDFs for energy dissipation rates, 4×10^8 data points are put into 2×10^4 bins along the ξ_n axis. We discarded those bins containing the number of data points less than 25. Note that the average number of data points per bin is 2×10^4 . In drawing the created PDFs for energy dissipation rates, not all the bins but nearly every 10^2 bins are plotted for better visibility. The experimental PDF in the region near the right-most end points are scattered because of the lower statistics due to smaller number of data points in the bins located there (see figure 1 (a) and figure 3 (a)).

The experimental PDF is analyzed with the help of the theoretical formula for PDF by the following procedure: (1) Pick up three experimental PDFs with consecutive r values, say, r_1 , $r_2 = r_1\delta$ and $r_3 = r_1\delta^2$. (2) With a trial μ value, analyze each of the three experimental PDFs to find out tentative but the best values q' , w_3 , θ , α^* and $n_i = \ln(r_i/\ell_0)/\ln \delta$ ($i = 1, 2, 3$) for the theoretical PDF. (3) Check if the differences $n_3 - n_2$ and $n_2 - n_1$ are close to 1 or not. (4) If not, change μ value, and repeat the processes (2) and (3) until one arrives at the set of best fit parameters under the condition $n_3 - n_2 = n_2 - n_1 \simeq 1$ within a settled accuracy. (5) With thus determined common μ value, determine the best fit values q' , w_3 , θ and α^* for each of other PDFs which are not picked out for the above processes (1) to (4). One notices that $n_i - n_{i-1} \simeq 1$ are satisfied automatically for every PDFs created from the experiment.

The PDFs of energy dissipation rates are analyzed in figure 1 for the magnification $\delta = 3$ on (a) log and (b) linear scale in the vertical axes. For better visibility, each PDF is shifted by appropriate unit along the vertical axis. Closed circles are the experimental data points for PDFs for the cases $r/\eta = 21.9, 65.7, 197$ and 591 from the smallest value

Table 2. Parameters of PDFs created by (a) the formula (12) and (b) the formula (13). For both cases, $\mu = 0.260$ ($(1 - q) \ln \delta = 0.393$, $\alpha_0 = 1.15$, $X = 0.310$) giving $q = 0.642$.

r/η	(a)					(b)				
	n	\tilde{n}	q'	w_3	θ	n	\tilde{n}	q'	w_3	θ
6.57	5.50	6.04	1.03	0.250	2.10	5.20	5.71	1.03	0.250	3.50
21.9	4.00	4.39	1.02	0.250	3.50	4.00	4.39	1.04	0.380	5.30
65.7	3.00	3.30	1.05	0.490	4.10	3.00	3.30	1.04	0.450	5.00
197	1.60	1.76	1.06	0.780	4.50	2.00	2.20	1.07	0.750	6.00
591	0.60	0.416	1.09	1.25	5.80	0.580	0.637	1.09	1.24	6.20

Table 3. Connection points between the central and the tail part PDFs created by (a) the formula (12) and (b) the formula (13). $\langle\langle \varepsilon \rangle\rangle = 7.98 \text{ m}^2 \text{ sec}^{-3}$.

r/η	(a)			(b)		
	α^*	$\varepsilon_n^*/\langle\langle \varepsilon \rangle\rangle$	ξ_n^*	α^*	$\varepsilon_n^*/\langle\langle \varepsilon \rangle\rangle$	ξ_n^*
6.57	0.750	4.53	3.30	0.750	4.17	3.56
21.9	0.700	3.74	3.56	0.550	7.22	5.24
65.7	0.500	5.20	5.25	0.500	5.20	6.25
197	0.280	3.54	13.6	0.300	4.66	13.2
591	0.180	1.72	16.0	0.180	1.69	15.3

(top) to the largest value (bottom) where r corresponds to ℓ_n . Solid lines represent the theoretical PDFs given by (8) with (9) and (10). The parameters necessary for the theoretical PDF of A&A model are determined as $(1 - q) \ln \delta = 0.393$, $\alpha_0 = 1.15$ and $X = 0.310$, which turn out to be independent of δ . Other parameters are listed in table 2 (a) and table 3 (a). We performed the same analyses for other magnifications, $\delta = 2$ and 5, and found that the extracted value $\mu = 0.260$ is common to three cases in which PDFs are created with the different values of magnification, i.e., $\delta = 2, 3, 5$. It means that, within the analysis of the energy dissipation rates, the turbulent system under consideration is characterized by the value $\mu = 0.260$ for the intermittency exponent as it should be.

The dependence of \tilde{n} , α^* and θ on r/η ($= \ell_n/\eta$) are given, respectively, in figure 2 (a), (b) and (c) by closed circles for $\delta = 2$, by closed squares for $\delta = 3$ and by closed triangles for $\delta = 5$, which are extracted from the series of PDFs derived through (12). The solid line in each figure, (a), (b) and (c), represents an empirical formula obtained from all the data points for $\delta = 2, 3$ and 5 by the method of least squares. These figures prove the correctness of the assumption that the fundamental quantities of turbulence are independent of δ . The value of q' is found to be about $q' = 1.05$ (see table 2 (a)). We found that w_3 is also independent of δ and has a common line $\log_{10} w_3 = 0.372 \log_{10}(r/\eta) + \log_{10} 0.112$. Note that the empirical formulae for \tilde{n} , α^* and θ is effective only for the region $r/\eta \gtrsim 2$ since θ should satisfy $\theta > 1$ (see figure 2 (c)). We observe that the parameters q' , θ , w_3 for the central part PDF and the connection point α^* have scaling behaviors in much wider region not restricted to inside of the inertial range.

How much \tilde{n} data points are scattered from the empirical formula (see figure 2 (a))

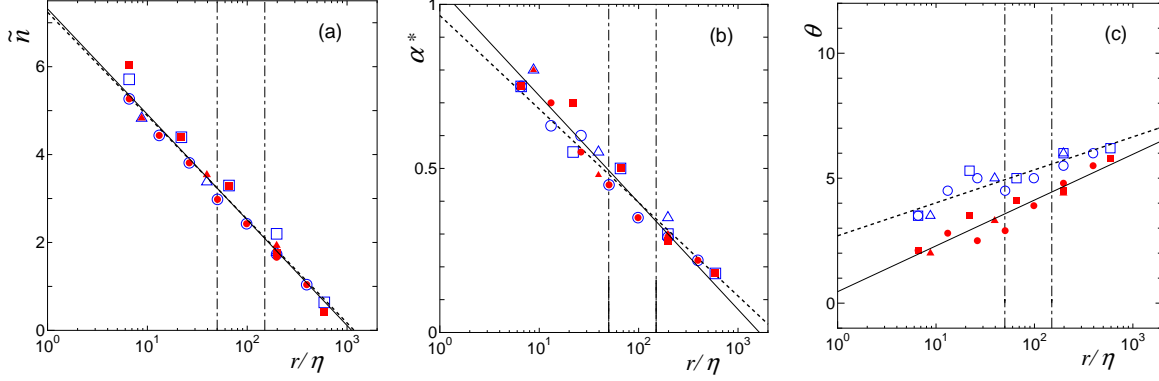


Figure 2. r/η ($= \ell_n/\eta$) dependence of (a) \tilde{n} , (b) α^* and (c) θ . In each figure, the data points extracted from the series of PDFs, which are created via (12) (via (13)), are plotted by closed (open) circles for $\delta = 2$, by closed (open) squares for $\delta = 3$, by closed (open) triangles for $\delta = 5$. Solid (dashed) lines are the empirical formulae (a) $\tilde{n} = -2.39 \log_{10}(r/\eta) + 7.31$ ($\tilde{n} = -2.36 \log_{10}(r/\eta) + 7.24$), (b) $\alpha^* = -0.326 \log_{10}(r/\eta) + 1.05$ ($\alpha^* = -0.285 \log_{10}(r/\eta) + 0.966$) and (c) $\theta = 1.83 \log_{10}(r/\eta) + 0.460$ ($\theta = 1.32 \log_{10}(r/\eta) + 2.70$) obtained from all the data points for $\delta = 2, 3$ and 5 . The inertial range is the region between the vertica

and also from the theoretical formula can be a measure how much we perform appropriate extraction of parameters and how much the experimental raw data include measurement errors. The data points for \tilde{n} in figure 2 (a) are scattered more compared with \tilde{n} for 4096³ DNS turbulence in figure 4 of Arimitsu N and T (2011), which may indicate that the time-series raw data for wind tunnel turbulence includes some indispensable measurement errors associated with readout processes. However, as the PDFs in figure 1 have higher enough resolution, i.e., smaller space between data points for PDFs, as mentioned before, we can extract the r/η -dependence of parameters in a good enough quality (compare figure 2 (c) for θ and figure 7 in Arimitsu N and T (2011)). There are some other differences. The value $\mu = 0.345$ for DNS turbulence is large compared with $\mu = 0.260$ for wind tunnel turbulence. The connection point α^* is constant for DNS ($\alpha^* = 0.800$) but has r/η -dependence around $\alpha^* \simeq 0.5$ for wind tunnel (see figure 2 (b)). On the other hand, q' is almost constant but has slight positive slope with respect to r/η for wind tunnel ($q' = 1.05$), while it has negative slope for DNS (the values are $q' \simeq 1.25$). It is an attractive future problem to find out the origin of the differences observed in these parameters taken from wind tunnel turbulence and DNS turbulence. It may be necessary to raise the number of data points of PDFs for 4096³ DNS beforehand for a much more precise comparison of wind tunnel and DNS turbulences.

4. Comparison of PDFs produced with full and less contaminations

In this section, we analyze the PDFs for the energy dissipation rates derived from the time-series data with the relation

$$\partial v / \partial t \simeq \Delta^{(0)} v / \Delta t = [v(t + \Delta t) - v(t)] / \Delta t \quad (13)$$

in order to study what difference comes out compared with the PDFs analyzed in section 3 which is derived by means of the relation (12). Note that the formula (13) estimates the values of velocity time derivative with $\Delta^{(0)} v / \Delta t$ which may contain full contamination, i.e., from the 1st order term with respect to Δt . We introduce the symbol $\varepsilon^{(0)}$ for the *local* energy dissipation rates derived from (13), i.e., $\varepsilon^{(0)} = 15\nu(\Delta^{(0)} v / \Delta t)^2 / 2U^2$.⁺ In creating the experimental PDFs for the energy dissipation rates, we took the same procedure as used in section 3.

We compare, in figures 3 (a) and (d)–(f), the PDFs of energy dissipation rates $\Pi_3^{(n)}(\varepsilon / \langle\langle \varepsilon \rangle\rangle)$ and $\Pi_3^{(n)}(\varepsilon^{(0)} / \langle\langle \varepsilon \rangle\rangle)$ which are created, respectively, with the help of formulae (12) and (13). Note that the arguments for every PDFs are scaled by $\langle\langle \varepsilon \rangle\rangle$ which does not depend on r ($= \ell_n$). In figure 3 (a) each PDF is displayed on log scale in vertical axis for the cases $r/\eta = 6.57$ (top), 21.9 (middle) and 65.7 (bottom), which are shifted by -2 unit along the vertical axis for better visibility. The magnification of their central part PDFs are displayed in figures 3 (d) $r/\eta = 6.57$, (e) 21.9 and (f) 65.7 on linear scale in vertical axis. The closed (open) circles and the full (dashed) lines are, respectively, the experimental and theoretical PDFs for $\Pi_3^{(n)}(\varepsilon / \langle\langle \varepsilon \rangle\rangle)$ ($\Pi_3^{(n)}(\varepsilon^{(0)} / \langle\langle \varepsilon \rangle\rangle)$) with $\mu = 0.260$. Note that the values of the intermittency exponent μ for $\Pi_3^{(n)}(\varepsilon / \langle\langle \varepsilon \rangle\rangle)$ and for $\Pi_3^{(n)}(\varepsilon^{(0)} / \langle\langle \varepsilon \rangle\rangle)$ turn out to be the same. Other parameters are listed in table 2 and table 3.

The relative differences $\Delta_n = [\Pi_3^{(n)}(\varepsilon^{(0)} / \langle\langle \varepsilon \rangle\rangle) - \Pi_3^{(n)}(\varepsilon / \langle\langle \varepsilon \rangle\rangle)] / \Pi_3^{(n)}(\varepsilon / \langle\langle \varepsilon \rangle\rangle)$ for $r/\eta = 6.57$ and 65.7 are given, respectively, in figures 3 (b) and (c), in which closed circles (full lines) represent experimental (theoretical) Δ_n . These figures show that the relative difference Δ_n in the region of central part of PDFs is about 10 times larger than the relative difference in the region of tail part.* The small but negative nearly constant values of Δ_n in the tail part region tells us that the tail of $\Pi_3^{(n)}(\varepsilon / \langle\langle \varepsilon \rangle\rangle)$ and that of $\Pi_3^{(n)}(\varepsilon^{(0)} / \langle\langle \varepsilon \rangle\rangle)$ are parallel with each other, which gives the reason why we obtained the same μ value for both PDFs. The relatively large error bars at the tail part may be attributed to the contaminations due to $\varepsilon^{(0)}$. The ε -dependence of Δ_n indicates that the central part of $\Pi_3^{(n)}(\varepsilon^{(0)} / \langle\langle \varepsilon \rangle\rangle)$ around its peak point moves to rightwards relative to the central part of $\Pi_3^{(n)}(\varepsilon / \langle\langle \varepsilon \rangle\rangle)$, whereas the tail part of the former PDF moves to leftwards relative to the tail part of the latter. The difference of the squared time derivatives with different contaminations is given by $(\Delta^{(0)} v / \Delta t)^2 - (\Delta^{(3)} v / \Delta t)^2 = (\partial v / \partial t)(\partial^2 v / \partial t^2)\Delta t + \mathcal{O}(\Delta t)^4$. From the direction of the relative horizontal shift of the

⁺ We observe that $\langle\langle \varepsilon^{(0)} \rangle\rangle = 8.08 \text{ m}^2 \text{ sec}^{-1}$ which is larger than $\langle\langle \varepsilon \rangle\rangle$.

* Note that the connection points of $\Pi_3^{(n)}(\varepsilon / \langle\langle \varepsilon \rangle\rangle)$ ($\Pi_3^{(n)}(\varepsilon^{(0)} / \langle\langle \varepsilon \rangle\rangle)$) for $r/\eta = 6.57$ and 65.7 locate, respectively, at $\varepsilon^* / \langle\langle \varepsilon \rangle\rangle = 4.06$ ($\varepsilon^{(0)*} / \langle\langle \varepsilon \rangle\rangle = 4.17$) and $\varepsilon^* / \langle\langle \varepsilon \rangle\rangle = 5.20$ ($\varepsilon^{(0)*} / \langle\langle \varepsilon \rangle\rangle = 5.20$).

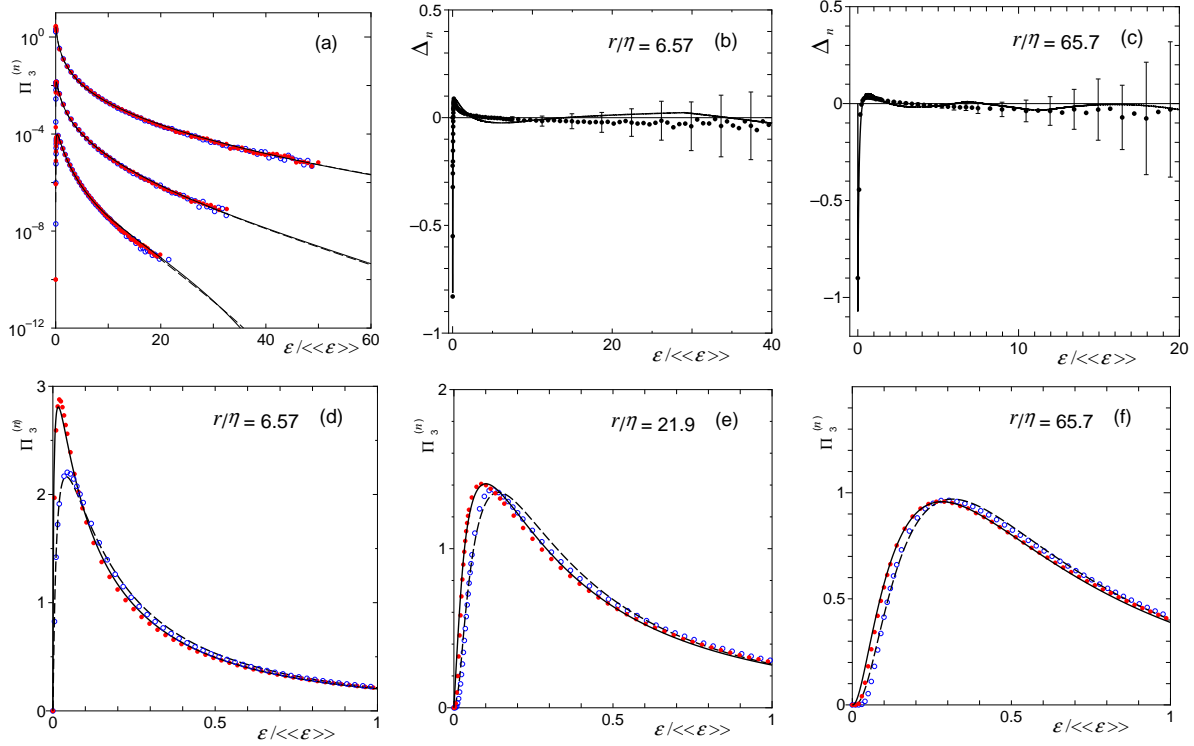


Figure 3. Comparison of PDFs for energy dissipation rates $\Pi_3^{(n)}(\varepsilon/\langle\langle\varepsilon\rangle\rangle)$ and $\Pi_3^{(n)}(\varepsilon^{(0)}/\langle\langle\varepsilon\rangle\rangle)$ created, respectively, with the formulae (12) and (13). In (a) and (d)–(f), closed (open) circles and full (dashed) lines are, respectively, the experimental and theoretical PDFs for $\Pi_3^{(n)}(\varepsilon/\langle\langle\varepsilon\rangle\rangle)$ ($\Pi_3^{(n)}(\varepsilon^{(0)}/\langle\langle\varepsilon\rangle\rangle)$) with $\mu = 0.260$. PDFs in (a) represent for the cases $r/\eta = 6.57$ (top), 21.9 (middle) and 65.7 (bottom), shifted by -2 unit along the vertical axis for better visibility. The magnification of the central part PDFs for each r ($= \ell_n$) is given in (d)–(f). The relative difference $\Delta_n = [\Pi_3^{(n)}(\varepsilon^{(0)}/\langle\langle\varepsilon\rangle\rangle) - \Pi_3^{(n)}(\varepsilon/\langle\langle\varepsilon\rangle\rangle)]/\Pi_3^{(n)}(\varepsilon/\langle\langle\varepsilon\rangle\rangle)$ is given for (b) $r/\eta = 6.57$ and (c) 65.7 , in which closed circles (full lines) are experimental (theoretical) Δ_n . Note that (a) and (b)–(f) are, respectively, drawn on log and linear scale in the vertical axes.

PDFs, we know that the net contributions of the velocity component v for the region around the peak point and of the tail region satisfy, respectively,

$$(\partial v/\partial t) (\partial^2 v/\partial t^2) > 0 \quad \text{and} \quad (\partial v/\partial t) (\partial^2 v/\partial t^2) < 0. \quad (14)$$

Taking into account the smallness of the gradient of tail part PDFs, we see that the absolute value of the latter in (14) is quite large compared with the former value.

The dependence of \tilde{n} , α^* and θ on r/η ($= \ell_n/\eta$) are given, respectively, in figure 2 (a), (b) and (c) by open circles for $\delta = 2$, by open squares for $\delta = 3$ and by open triangles for $\delta = 5$, which are extracted from the series of PDFs derived through (13). The dashed line in each figure, (a), (b) and (c), represents an empirical formula obtained from all the data points for $\delta = 2, 3$ and 5 by the method of least squares. These figures prove again, even for the case of full contamination, the correctness of the assumption that the fundamental quantities of turbulence are independent of δ . We also found that w_3 is independent of δ and has a common line $\log_{10} w_3 = 0.318 \log_{10} (r/\eta) + \log_{10} 0.141$.

The value of q' is found to be about $q' = 1.05$ (see table 2 (b)).

There is only a slightly visible difference of the lines for \tilde{n} , α^* , w_3 and of the values q' between those obtained from the two kinds of PDFs, one with less contamination and the other with full contamination (see figure 2 (a) and (b); see also table 2 and table 3). The significant difference appears in the r/η dependence of θ which are shown in figure 2 (c). The difference in θ explains the shift of the peak points of PDFs (see figures 3 (b)–(f)).

5. Summary and Discussions

The new scaling relation (2) is fundamental for the parameters α_0 , X and q , associated with the tail part PDF, to be determined self-consistently and to be independent of the magnification rate δ . It has been revealed that the scaling relation is intimately related to the marginal instabilities within a dynamical system at the δ^k -period ($\delta > 2$) saddle-node bifurcation points ($k = 1, 2, 3, \dots$) associated with δ^k -period windows constituting a self-similar nesting structure, which should be an origin of intermittent coherent motion in fully developed turbulence (Motoike and Arimitsu 2012). On the other hand, as there is no physical insight to determine the shape of the central part PDF yet, we introduced the trial function (11) to analyze the experimental PDFs, and tried to extract information to understand physically the incoherent fluctuating motion specific to turbulent system with the help of the behaviors of parameters q' , w_3 and θ , associated with the trial function. The connection point ξ_n^* , or equivalently α^* or ε_n^* , between the central and tail parts of PDF provides us with an important information to distinguish the characteristics of the two element of fluid motions constituting turbulence.

The independence of \tilde{n} from δ ensures the uniqueness of the PDF of α for any value of δ . The comparison between the empirical formulae for \tilde{n} given in figure 2 (a) and the theoretical formula (6) provides us with the estimation $\ell_0 = 20.6$ cm which is about the same as the correlation length 17.9 cm given in table 1.‡ Here, we are assuming that the empirical formulae are effective even for $r/\eta \lesssim 2$ (see the discussion in section 3 about the effective region of r/η). Note that ℓ_0 gives an estimation of the diameter of the largest eddy within the energy cascade model.

The connection point α^* is adjusted in order for the best fit of the PDF around the region between the peak and the connection point. Note that the region $\alpha \leq \alpha^*$ ($\alpha > \alpha^*$) corresponds to the tail (central) part of the PDF. It is revealed that the value α^* satisfies $\alpha^* \lesssim 0.75$ for all the data points with different values of r/η (see figure 3), which proves the assumption that the central part $\hat{\Pi}_{3,cr}^{(n)}(\xi_n)$ is constituted of two contributions, one from the coherent contribution $\Pi_{3,S}^{(n)}(\varepsilon_n)$ and the other from the incoherent contribution $\Delta\Pi_3^{(n)}(\varepsilon_n)$, and that almost all the contribution to the tail part $\hat{\Pi}_{3,tl}^{(n)}(\xi_n)$ comes from the coherent motion of turbulence. Remember that the energy dissipation rate becomes singular for $\alpha < 1$.

‡ The estimated value for ℓ_0 is also about the same as the separation 20 cm of the axes of adjacent rods forming the grid placed in the wind tunnel.

As for the parameters appeared in the trial function for the central part PDFs, $\exp[-g(\xi_n)]$ in (11), the discoveries that $q' \simeq 1.05$ and that θ and $\ln w_3$ reveal scaling properties are quite attractive for the research looking for the nature of the fluctuations surrounding the coherent turbulent motion of fluid. The fact that the value q' is quite close to 1 indicates that the HCT type function in (11), i.e., the part giving $\exp[-g(\xi_n)](\xi_n^*/\xi_n)^{\theta-1}$, is close to an exponential function. There is no theoretical prediction yet, which is based on an ensemble theoretical aspect or on a dynamical aspect starting with the N-S equation, to produce the formula for the central part PDF that represents the contributions both of the coherent turbulent motion providing intermittency and of incoherent fluctuations (background flow) around the coherent motion. If one could succeed to formulate a dynamical theory which produces properly the formula for the central part of PDFs starting with the N-S equation, it may provide us with an appropriate pathway to the dynamical approach, e.g., the renormalization group approach, to fully developed turbulence. A study to this direction is in progress.

Introducing two difference formulae (12) and (13) for the estimate of $\partial v/\partial t$, i.e., $\Delta^{(3)}v/\Delta t$ with less contamination and $\Delta^{(0)}v/\Delta t$ with full contamination, we performed a trial for the extraction of information from PDFs by comparing two kinds of PDFs for energy dissipation rates, $\Pi_3^{(n)}(\varepsilon/\langle\langle\varepsilon\rangle\rangle)$ and $\Pi_3^{(n)}(\varepsilon^{(0)}/\langle\langle\varepsilon\rangle\rangle)$ with $\varepsilon \propto (\Delta^{(3)}v/\Delta t)^2$ and $\varepsilon^{(0)} \propto (\Delta^{(0)}v/\Delta t)^2$. We observed that the intermittency exponents for the two kinds of PDFs turn out to take the same value $\mu = 0.260$ (see table 2 and table 3 for other parameters). Through the accurate analyses of PDFs, it was also revealed that the parameters for $\Pi_3^{(n)}(\varepsilon/\langle\langle\varepsilon\rangle\rangle)$ and $\Pi_3^{(n)}(\varepsilon^{(0)}/\langle\langle\varepsilon\rangle\rangle)$ are independent of δ thanks to the new scaling relation (2), and that they show quite similar scaling behaviors extending to the regions with smaller and larger r/η values outside the inertial range (see figure 2). We observed that the parameters μ and \tilde{n} controlling the tail parts of the two kinds of PDFs coincide with each other within the present accuracy (see table 2 and figure 2 (a)). The connection points α^* of the tail and central parts of the PDFs take almost the same value for each r/η (see table 3 and figure 2 (b)). It is found that, among the parameters controlling the central part, only θ has a relatively larger deviation between the two different PDFs (see table 2 and figure 2 (c)), which is related to the sift of the peak point occurred between the two kinds of PDFs. Other parameters q' and w_3 do not have significant difference among the two PDFs (see table 2).

The relative difference Δ_n between $\Pi_3^{(n)}(\varepsilon^{(0)}/\langle\langle\varepsilon\rangle\rangle)$ and $\Pi_3^{(n)}(\varepsilon/\langle\langle\varepsilon\rangle\rangle)$ (see figure 3) provides us with the information (14). It seems to tell us that the net behavior of incoherent motion of fluid contributing mainly around the peak point (central part) of PDF is an *unstable* time-evolution, whereas that of coherent turbulent motion contributing mainly to the tail part of PDF is a *stable* time-evolution. Further investigation about these outcomes and their interpretation is necessary, which we leave as one of the attractive future problems.††

†† We observed that there is no visible difference between $\Pi_3^{(n)}(\varepsilon/\langle\langle\varepsilon\rangle\rangle)$ and the PDF extracted with the formula $\partial v/\partial t \simeq [v(t+\Delta t) - v(t-\Delta t)]/2\Delta t$ which is correct without contamination up to the term of $\mathcal{O}(\Delta t)$.

There are differences in value and/or in r/η -dependence between the parameters associated with central part of PDFs for wind tunnel turbulence and those for DNS turbulence. We will perform the precise comparison between them by raising the resolution of PDFs for 4096^3 DNS by creating more data points for PDFs with respect to r/η , and to present the results elsewhere in the near future.

Acknowledgments

The authors (T.A. and N.A.) would like to thank Prof. T. Motoike, Dr. K. Yoshida, Mr. M. Komatsuzaki and Mr. K. Takechi for fruitful discussions.

References

- Aoyama T, Ishihara T, Kaneda Y, Yokokawa M, Itakura K and Uno A 2005 Statistics of energy transfer in high-resolution direct numerical simulation of turbulence in a periodic box *J. Phys. Soc. Jpn.* **74** 3202–3212
- Arimitsu N and Arimitsu T 2002 Multifractal analysis of turbulence by using statistics based on non-extensive Tsallis' or extensive Rényi's entropy *J. Korean Phys. Soc.* **40** 1032–1036
- Arimitsu N and Arimitsu T 2011 Verification of the scaling relation within MPDFT by analyzing PDFs for energy dissipation rates out of 4096^3 DNS *Physica A* **390** 161–176
- Arimitsu T and Arimitsu N 2000a Analysis of Fully Developed Turbulence in terms of Tsallis Statistics *Phys. Rev. E* **61** 3237–3240
- Arimitsu T and Arimitsu N 2000b Tsallis statistics and fully developed turbulence *J. Phys. A: Math. Gen.* **33** L235–L241 [CORRIGENDUM: 2001 **34** 673–674]
- Arimitsu T and Arimitsu N 2001 Analysis of turbulence by statistics based on generalized entropies *Physica A* **295** 177–194
- Arimitsu T and Arimitsu N 2002 PDF of velocity fluctuation in turbulence by a statistics based on generalized entropy *Physica A* **305** 218–226
- Arimitsu T and Arimitsu N 2011 Analysis of PDFs for energy transfer rates from 4096^3 DNS — Verification of the scaling relation within MPDFT *J. Turbulence* **12** 1–25
- Benzi R, Paladin G, Parisi G and Vulpiani A 1984 On the multifractal nature of fully developed turbulence and chaotic systems *J. Phys. A: Math. Gen.* **17** 3521–3531
- Benzi R, Biferale L, Paladin G, Vulpiani A and Vergassola M 1991 Multifractality in the statistics of the velocity gradients in turbulence *Phys. Rev. Lett.* **67** 2299–2302
- Biferale L, Boffetta G, Celani A, Devenish B J, Lanotte A and Toschi F 2004 Multifractal statistics of Lagrangian velocity and acceleration in turbulence *Phys. Rev. Lett.* **93** 064502-1-4
- Biferale L and Procaccia I 2005 Anisotropy in Turbulent Flows and in Turbulent Transport *Phys. Rep.* **414** 43–164
- Chevillard L, Castaing B, Lévêque E and Arneodo A 2006 Unified multifractal description of velocity increments statistics in turbulence: Intermittency and skewness *Physica D* **218** 77–82
- Cleve J, Greiner M and Sreenivasan K R 2003 On the effects of surrogacy of energy dissipation in determining the intermittency exponent in fully developed turbulence *Europhys. Lett.* **61** 756–761
- Costa U M S, Lyra M L, Plastino A R and Tsallis C 1997 Power-law sensitivity to initial conditions within a logistic-like family of maps: Fractality and nonextensivity *Phys. Rev. E* **56** 245–250
- Dubrulle B 1994 Intermittency in fully developed turbulence: log-Poisson statistics and generalized scale covariance *Phys. Rev. Lett.* **73** 959–962
- Grassberger P 1983 Generalized dimension of strange attractors *Phys. Rev. Lett. A* **97** 227–229
- Halsey T C, Jensen M H, Kadanoff L P, Procaccia I and Shraiman B I 1986 Fractal measures and their singularities: The characterization of strange sets *Phys. Rev. A* **33** 1141–1151

- Havrda J H and Charvat F 1967 Quantification methods of classification processes: Concepts of structural α entropy *Kybernetika* **3** 30–35
- Hentschel H G E and Procaccia I 1983 The infinite number of generalized dimensions of fractals and strange attractors *Physica D* **8** 435–444
- Hosokawa I 1991 Turbulence models and probability distributions of dissipation and relevant quantities in isotropic turbulence *Phys. Rev. Lett.* **66** 1054–1057
- Lyra M L and Tsallis C 1998 Nonextensivity and multifractality in low-dimensional dissipative systems *Phys. Rev. Lett.* **80** 53–56
- Mandelbrot B B 1974 Intermittent turbulence in self-similar cascades: Divergence of high moments and dimension of the carrier *J. Fluid Mech.* **62** 331–358
- Meneveau C and Sreenivasan K R 1987 The multifractal spectrum of the dissipation field in turbulent flows *Nucl. Phys. B (Proc. Suppl.)* **2** 49–76
- Motoike T and Arimitsu T 2012 in preparation to submit
- Mouri H, Hori A and Takaoka M 2008 Fluctuations of statistics among subregions of a turbulence velocity field *Phys. Fluids* **20** 035108–1–6
- Nelkin M 1990 Multifractal scaling of velocity derivatives in turbulence *Phys. Rev. A* **42** 7226–7229
- Parisi G and Frisch U 1985 *Turbulence and predictability in geophysical fluid dynamics and climate dynamics* (New York: North-Holland/American Elsevier) pp 84–87
- Rényi A 1961 On measures of entropy and information *Proc. of the 4th Berkeley Symp. on Mathematical Statistics and Probability* (Berkeley: USA) pp 547–561
- She Z-S and Leveque E 1994 Universal scaling laws in fully developed turbulence *Phys. Rev. Lett.* **72** 336–339
- She Z-S and Waymire E C 1995 Quantized energy cascade and log-Poisson statistics in fully developed turbulence *Phys. Rev. Lett.* **74** 262–265
- Suyari H and Wada T 2006 Scaling property and Tsallis entropy derived from a fundamental nonlinear differential equation *Proc. of the 2006 Int. Symp. on Inf. Theory and its Appl.* (ISITA2006) pp 75–80 (*Preprint* cond-mat/0608007)
- Tsallis C 1988 Possible generation of Boltzmann-Gibbs statistics *J. Stat. Phys.* **52** 479–487
- Tsallis C 2001 Nonextensive statistical mechanics and thermodynamics: Historical background and present status *Nonextensive Statistical Mechanics and Its Applications* ed S Abe and Y Okamoto (Berlin: Springer-Verlag) pp 3–98